# Task-Dependent V1 Responses in Human Retinitis Pigmentosa

*Yoichiro Masuda,*[1,2] *Hiroshi Horiguchi,*[1,2,3] *Serge O. Dumoulin,*[4] *Ayumu Furuta,*[5] *Satoru Miyauchi,*[6] *Satoshi Nakadomari,*[1,7] *and Brian A. Wandell*[3]

**Purpose.** During measurement with functional MRI (fMRI) during passive viewing, subjects with macular degeneration (MD) have a large unresponsive lesion projection zone (LPZ) in V1. fMRI responses can be evoked from the LPZ when subjects engage in a stimulus-related task. The authors report fMRI measurements on a different class of subjects, those with retinitis pigmentosa (RP), who have intact foveal vision but peripheral visual field loss.

**Methods.** The authors measured three RP subjects and two control subjects. fMRI was performed while the subjects viewed drifting contrast pattern stimuli. The subjects passively viewed the stimuli or performed a stimulus-related task.

**Results.** During passive viewing, the BOLD response in the posterior calcarine cortex of all RP subjects was in phase with the stimulus. A bordering, anterior LPZ could be identified by responses that were in opposite phase to the stimulus. When the RP subjects made stimulus-related judgments, however, the LPZ responses changed: the responses modulated in phase with the stimulus and task. In control subjects, the responses in a simulated V1 LPZ were unchanged between the passive and the stimulus-related judgment conditions.

**Conclusions.** Task-dependent LPZ responses are present in RP subjects, similar to responses measured in MD subjects. The results are consistent with the hypothesis that deleting the retinal input to the LPZ unmasks preexisting extrastriate feedback signals that are present across V1. The authors discuss the implications of this hypothesis for visual therapy designed to replace the missing V1 LPZ inputs and to restore vision. (*Invest Ophthalmol Vis Sci.* 2010;51:5356–5364) DOI:10.1167/iovs.09-4775

From the [1]Department of Ophthalmology, Jikei University, School of Medicine, Tokyo, Japan; [3]Department of Psychology, Stanford University, Stanford, California; [4]Helmholtz Institute, Experimental Psychology, Utrecht University, Utrecht, Netherlands; [5]Maeda Ophthalmic Clinic, Fukushima, Japan; [6]Kobe Advanced ICT Research Center, National Institute of Information and Communications Technology, Kobe, Japan; and [7]Department of Functional Training III, National Rehabilitation Center for Persons with Disabilities, Tokorozawa, Japan.

[2]These authors contributed equally to the work presented here and should therefore be regarded as equivalent authors.

Supported by Larry L. Hillblom Foundation Fellowship 2005/2BB (SOD), Grant-in-Aid for JSPS Fellows 20.11472 (HH), and National Eye Institute Grant EY03164 (BW).

Submitted for publication October 14, 2009; revised February 11 and April 7, 2010; accepted April 13, 2010.

Disclosure: **Y. Masuda**, None; **H. Horiguchi**, None; **S.O. Dumoulin**, None; **A. Furuta**, None; **S. Miyauchi**, None; **S. Nakadomari**, None; **B.A. Wandell**, None

Corresponding author: Yoichiro Masuda, Department of Ophthalmology, Jikei University, School of Medicine, 3-25-8 Nishi-Shinbashi, Minato-Ku, Tokyo, 105-8461, Japan; massuuu@gmail.com.

Cortical responses to visual stimuli in primary visual cortex (V1) of subjects with macular degeneration (MD) differ from responses in control subjects in two significant ways. First, under passive viewing conditions, MD subjects have large unresponsive zones corresponding to the lesion projection zone (LPZ) of the retinal damage.[1–4] A second difference between the MD subjects and controls concerns the V1 responses when subjects perform a stimulus-related task. Under these conditions, the V1 responses in controls with a simulated scotoma are consistent with the basic retinal projection zones determined by retinotopic mapping. In the juvenile macular degeneration (JMD) subjects, however, the task-related responses in V1 appear to spread beyond the normal projection zone into the LPZ.[2] Performing a task spreads the V1 response in the JMD subjects but not in controls.

There are many alternative hypotheses concerning the effects of retinal lesions on V1, and the extent of V1 adult cortical plasticity remains controversial.[3] Because human measurements are concentrated on a limited number of subjects with macular loss, we may learn more by extending the measurement to subjects with a different retinal dystrophy: retinitis pigmentosa (RP). These subjects have visual field contraction; that is, they have peripheral visual field loss but relatively intact central vision and foveal function. In this report, we examine whether the hypothesis of a signal imbalance also applies to the LPZ responses in RP subjects.

## Subjects, Materials, and Methods

Data were acquired at two sites, the National Institute of Information and Communications Technology (NICT; Tokyo, Japan) and Stanford University (Stanford, CA). There were slight differences in the methodology, but the results from the two sites were in excellent agreement. When the methods differed, we specified the settings.

### Subjects

We report measurements from five subjects. Three subjects have RP (RP1–3; for details, see Supplementary Table S1, http://www.iovs.org/cgi/content/full/51/10/5356/DC1); two control subjects have normal vision (C1–2). RP is an inherited progressive degeneration.[5–8] Rod photoreceptors deteriorate first, followed by cone photoreceptors. The age of onset is variable, ranging from birth to mid-adulthood. Typical symptoms of RP include night blindness (nyctalopia) followed by decreasing visual fields and finally a loss of central vision. Most patients are legally blind by age 40 because of severely constricted visual fields. The diagnosis of RP is based on clinical history, fundus examination, visual field measurement, and electroretinogram.

For the fMRI experiments, all RP subjects were measured through the eye that had higher acuity.

RP1 (male, age 37) was diagnosed at age 21. The subject viewed the stimuli with his left eye, and a patch covered his right eye. His



Investigative Ophthalmology & Visual Science, October 2010, Vol. 51, No. 10

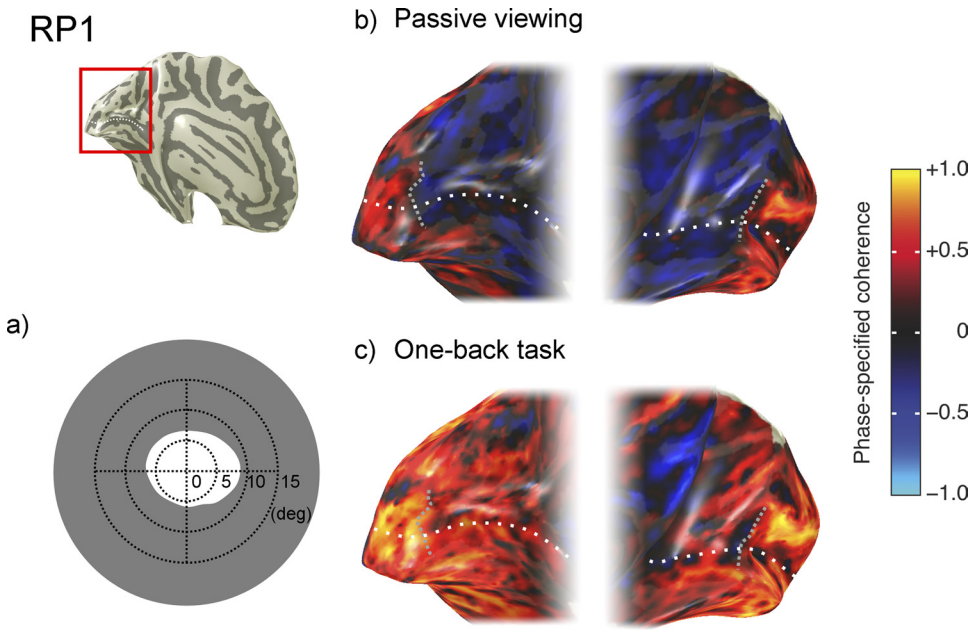


**FIGURE 1.** Task-dependent BOLD responses in an RP subject (RP1). (**a**) Schematic diagram of the visual field (left eye). *Dark gray*: regions of absolute visual field loss. (**b**) Phase-specified coherence map measured during passive viewing. *Upper left*: coherence is shown on an inflated representation of occipital cortex. *White dotted line*: calcarine sulcus. Positive and negative values indicate responses that are in-phase (*orange*, *yellow*) or out of phase (*blue*) with the stimulus. The border between the positive and negative responses in calcarine (*gray dashed line*) separates the lesion projection zone (LPZ, anterior) and functional projection zone (FPZ, posterior) (**c**) During the OBT, the coherence becomes positive in both the LPZ and the FPZ.

contracted visual field was approximately 16 × 13° in diameter in the measured eye (Fig. 1a). In the fMRI experiments, he fixated using his fovea.

The visual field regions in RP1 with peripheral visual field loss are shown in Figure 1a. Absolute visual field loss is defined as those regions in visual space where the subject fails to detect the highest contrast and largest size Goldmann perimetry stimulus (size V).

RP2 (male, age 30) was diagnosed at age 16. His visual field was narrow, and he had nyctalopia as an infant; presumably RP onset occurred during infancy. He did not notice progression of the visual field disturbance from infancy. The subject viewed the stimuli with his right eye, and a patch covered the left eye. His contracted visual field was approximately 15 × 15° in diameter in the measured eye (see Fig. 5). In the fMRI experiments, he fixated using his fovea.

RP3 (male, age 38) was diagnosed at age 6, with slow progression until age 17. The right eye is almost blind. During the fMRI measurements, he viewed the stimulus with his left eye, and the right eye was covered with a patch. His contracted visual field spanned approximately 12 × 13° diameter in the measured eye (see Fig. 5). During the fMRI experiments, he fixated using his fovea.

C1 (male, age 35) maintained fixation and in different experiments was presented with stimuli that simulated the visual field loss of either RP1 or RP3; that is, the stimuli were presented within the contracted visual field of either RP1 or RP3 (Fig. 2a). C2 (male, age 30) was presented with stimuli corresponding to the loss of RP3; that is, the stimuli fell on a part of the retina corresponding to the location of the contracted visual field of RP3. Like RP1 and RP3, the control subjects used their left eye only and a patch covered the right eye.

We refer to the V1 region that during passive viewing responds in synchrony with the central stimulation as the functional projection zone (FPZ). The V1 region anterior to the FPZ, in which the fMRI is negative or absent, is the LPZ.

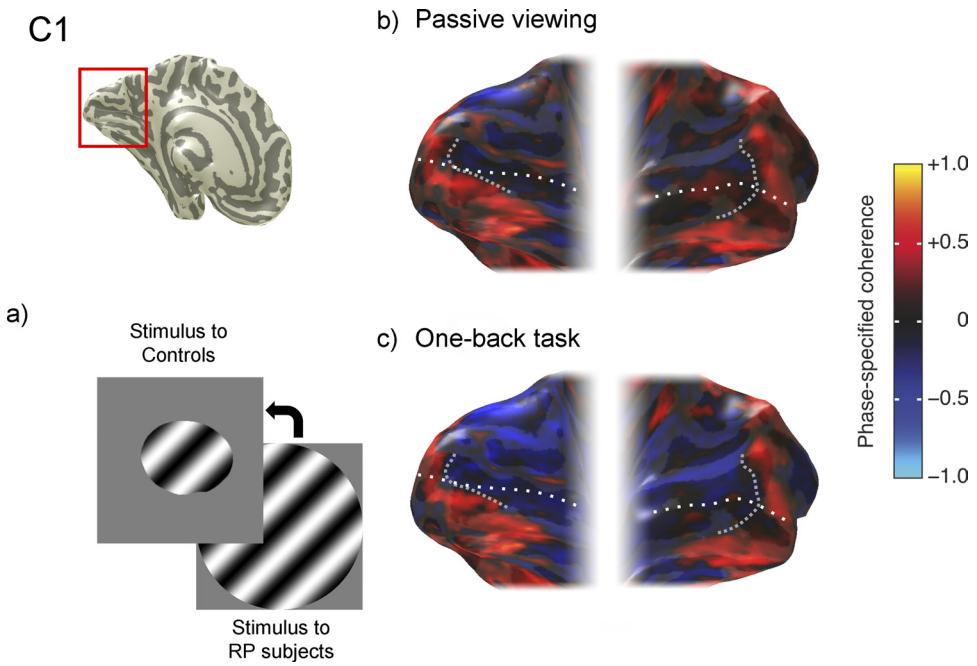


**FIGURE 2.** Absence of task-dependent BOLD responses in a control subject. (**a**) Contrast stimulus shown to C1 covers the functional portion of the visual field in RP1 (left eye). (**b**) Phase-specified coherence map in the passive viewing condition. (**c**) Phase-specified coherence map in the OBT is almost identical with that in passive viewing. Other details as in Figure 1.

The data from subjects RP1, RP2, and C1 were acquired at NICT. Subjects RP3, C1, and C2 were measured at Stanford University. All procedures adhered to protocols based on the World Medical Association Declaration of Helsinki ethical principles for medical research involving human subjects and were approved by the ethical committees of NICT and Stanford University. All subjects provided written informed consent to participate in the project.

## Visual Field Perimetry

The visual fields of RP1 and RP2 were measured by Goldmann perimetry. We used kinetic targets and defined the absolute visual field loss as the region in which they could not detect the highest contrast and largest size stimulus (size V, 1.72° diameter). For subject RP3, we measured the visual field deficit using custom software[2] implemented with PsychToolbox.[9,10] In this experiment, the stimuli were dots (1.72° diameter) on a gray background that was 0.5 log unit lower than the target dot. These settings are comparable to the standard Goldmann perimetry size V and comparable to standard Humphrey perimetry at settings designed to detect absolute visual field loss. While maintaining fixation, the subject indicated whether he perceived a brief stimulus presentation of 0.05 second.

The purpose of these perimetry measurements was to establish the region of the peripheral visual field loss. The kinetic Goldman perimetry measurement is a very sensitive test; RP1 and RP2 had no sensitivity to these targets. The custom software is also sensitive and is similar to the Humphrey visual field measurement. Using Goldman kinetic perimetry in RP3 might have produced a preserved visual field slightly larger than the one shown (see Fig. 5). This would not have altered any conclusions in this study.

## MR Stimuli

The visual stimuli consisted of drifting contrast patterns that spanned 28° diameter. At Stanford, there were four stimulus cycles of the stimulus drifting at a rate of 14°/s; at NICT, there were two stimulus cycles of the stimulus drifting at a rate of 23.2°/s. Hence, the temporal flicker rate was 2 Hz (Stanford) or 1.66 Hz (NICT). Throughout the fMRI measurements, all subjects maintained fixation using their fovea at a dot (0.7° diameter) placed at the center of the stimulus. In control subjects, the size of the stimulus extent was restricted to the extent of the functional visual fields of RP1 or RP3.

Stimuli were presented in a block design between alternating blocks showing the drifting contrast patterns and uniform gray field (mean luminance). The duration of each block was 12 (Stanford) or 15 (NICT) seconds. During the blocks with drifting contrast patterns, contrast images were presented for 750 ms and 250 ms blank (Stanford) or 800 ms contrast and 200 ms blank (NICT) repeatedly. The motion direction of the drift changed randomly between presentations. Each session contained 6 (Stanford) or 10 (NICT) stimulus blocks.

Two different task conditions were used. In the passive viewing condition, subjects viewed stimuli passively (no task). In the one-back task (OBT) condition, the subjects reported when they saw two consecutive repetitions of the same stimulus (drifting-contrast pattern). Subjects performed the task well; during the OBT, correct response rates were nearly 100%. The stimuli were the same for both conditions. The two tasks were interleaved within a session but not within a single scan.

At NICT, the stimuli were presented using a projector (D-ILA; DLA-G150; Victor Company of Japan, Yokohama, Japan) and publicly provided software (Visual Basic 6.0, Direct X 7.0; Microsoft, Redmond, WA). At Stanford, the stimuli were generated in the Matlab programming environment (MathWorks; Matlab, Natick, MA) using the PsychToolbox[9,10] on a laptop computer (G4 Powerbook; Macintosh; Apple, Cupertino, CA) and presented using an LCD projector (LT158; NEC, Santa Clara, CA). Subjects viewed the display through a mirror mounted above the head.

## Scanning Procedure

Images were acquired for NICT as follows: fMRI data of RP1, RP2, and C1 were acquired on a scanner (3-T Trio; Siemens, Erlangen, Germany). fMRI images (T2*-weighted BOLD, responses) were collected parallel to the AC-PC line through the occipital lobes using a single-shot gradient echo planer imaging sequence (37 planes; TR/TE, 3000/36 ms; flip angle, 90°; voxel size, 2 × 2 × 2 mm; FOV, 192 mm). An infrared-video eye-monitoring system (ST-661; NAC Image Technology, Tokyo, Japan) was used to observe fixation stability. This eye-monitoring system confirmed that all subjects were able to maintain stable fixation for the duration of the experimental runs. Precise fixation is not important for these measurements; moving the eye does not shift the relationship between the retinal lesion and its cortical projection zone. The only requirement is that eye fixations be small enough so that the very large stimulus covers the healthy retina.

Images were acquired for Stanford as follows: fMRI data of RP3 and the controls (C1–2) were acquired on a scanner (3-T; General Electric, Milwaukee, WI). fMRI images (T2*-weighted BOLD responses) were collected orthogonally to the calcarine sulcus using a two-dimensional spiral sequence (TR/TE, 1500/30 ms; flip angle, 55°; effective voxel resolution, 2.5 × 2.5 × 3 mm).[11,12]

A high-resolution anatomic $T_1$-weighted MRI volume scan of the entire head was also obtained for each subject (1 mm isotropic).

## Data Analysis and Visualization

Data were analyzed using the mrVista software (Stanford, http://white.stanford.edu/software).[13] The first 10 time frames in each functional run were discarded because of start-up magnetization transients in the data. The remaining time frames were corrected for motion.[14] No spatial smoothing was performed. The fMRI signals were converted to percentage signal change by dividing and subtracting each voxel's time series by the time-series mean. Baseline drifts were removed from the time series by high-pass temporal filtering.

We measured the strength of the BOLD responses by calculating the phase-specified coherence of each fMRI time series.[15–17] This quantity measures the amplitude of the BOLD response at the stimulus frequency and phase, adjusted for the hemodynamic delay. The hemodynamic delay is estimated in each subject from the positive BOLD responses. The precise formula for the phase-specified coherence is given in Masuda et al.[2] The values ranged between −1 and 1; positive values reflect stronger responses to the drifting contrast, and negative values reflect stronger responses to the uniform background. We denote the in-phase and out-of-phase response with stimulus as a positive or a negative BOLD response, respectively. We estimate the stimulus-driven phase of the fMRI time course from the time course data with which the most reliable activations were found, usually near the occipital pole. The data had no absolute baseline; there was only a measure of the BOLD response modulation as the stimulus contrast turned on and off.

Gray matter was segmented from the high-resolution anatomic volume for each subject, rendered in three dimensions close to the white matter boundary and unfolded using publicly available software.[13,18] Activations were visualized on the inflated representation of the white-gray matter boundary.

# Results

## Task-Dependent Stimulus-Synchronized Responses in LPZ

The response coherence during passive viewing (Fig. 1b) and OBT (Fig. 1c) is shown on an inflated cortical surface of the posterior hemispheres of RP1. In posterior regions of both hemispheres, there was a strong positive response (in-phase with the stimulus) in V1 and nearby extrastriate cortex. The response spanned the occipital pole and extended forward several centimeters. There were also positive responses on

most of the ventral occipital cortex, a region that has a central visual field bias.[19–22]

Within V1, the positive response extended in an anterior direction along the calcarine sulcus, a distance consistent with the expected response given the preserved central visual field (Fig. 1a). At a boundary approximately 2 cm anterior to the occipital pole, the responses in V1, V2, and V3 became negative (out-of-phase with the stimulus). The boundary between positive and negative BOLD response during passive viewing was marked on the images (Figs. 1b 1c); we defined the LPZ as the region anterior to this boundary.

When the RP subject was presented with the same stimulus but engaged in a OBT, the response pattern changed significantly (Fig. 1c). The coherence of the in-phase responses increased throughout visual cortex, and the negative LPZ responses became positive. Given that the stimulus was the same in both conditions, we attributed the increased activation in the LPZ to the change in task demands.

These data show that a subject with preserved macular function has the same task-dependent spread of activation into the LPZ as MD subjects.[2]

The responses in a control subject measured under the same conditions, but with a simulated peripheral visual field loss (Fig. 2a), showed a different pattern. For the control subject, task performance did not change the spatial distribution of the BOLD response (Figs. 2b, 2c).

## Time Series Measurements along the Calcarine

We examined the time series of the BOLD response in calcarine cortex of RP1 (Fig. 3) and selected nine circular regions of interest (ROIs; each 5-mm radius) from the occipital pole toward the anterior calcarine. The first ROI was centered on the boundary that divides the positive and the negative BOLD responses. Eight additional ROIs were positioned in the fundus of the calcarine sulcus (Fig. 3a). Four ROIs were placed in anterior and four in posterior calcarine. The center of each ROI was placed on the border of an adjacent ROI (5-mm center-to-center spacing). The collection of nine ROIs in each hemisphere spanned 5 cm (edge-to-edge) or 4 cm (center-to-center) (Figs. 3a, 4 inset).

Average single-cycle BOLD time series during passive measurements are shown in Figure 3b. The surface represents the combination of the BOLD time series from all nine ROIs averaged between both hemispheres. The contrast stimulus was presented in the first half of the cycle and was replaced by a uniform field after 15 seconds. The four ROIs near the occipital pole showed a positive BOLD response to the stimulus. Beyond the boundary, at the fifth ROI, the BOLD responses became negative. During the OBT, the BOLD time series amplitudes in the FPZ (posterior ROIs) increased, and the amplitudes in the LPZ (anterior ROIs) changed from negative to positive (Fig. 3c).

We repeated the time series analysis in two control subjects, adjusting the stimulus to simulate the contracted visual field. In the control subjects, the average single-cycle BOLD time series did not change between passive and one-back viewing conditions (Fig. 4). In subject C1, the responses in passive and active viewing were similar. In subject C2, there was a task-dependent increase in the BOLD response of the central visual field. Adding the task did not significantly influence the negative BOLD response in the LPZ in either control subject.

We measured BOLD time series in two additional subjects with RP (Fig. 5). Similar to the analysis in RP1, we identified the border between the positive and the negative BOLD responses during passive viewing in each subject. We created nine ROIs and plotted the average, single-cycle time series on both sides of this border (Fig. 5). In passive viewing, there was a negative BOLD response in the anterior calcarine that typically represented the peripheral visual field (Fig. 5a). In both RP2 and RP3, the OBT increased the responses in the ROIs anterior to the border, changing the responses from negative to positive BOLD (Fig. 5b). This increase in the LPZ was not as large as the increase observed in RP1 (Fig. 3bc).

We have plotted the BOLD time series from the LPZ ROIs and additional statistical analyses of the LPZ responses in Supplementary Figures S1 and S2, respectively (http://www.iovs.org/cgi/content/full/51/10/5356/DC1).

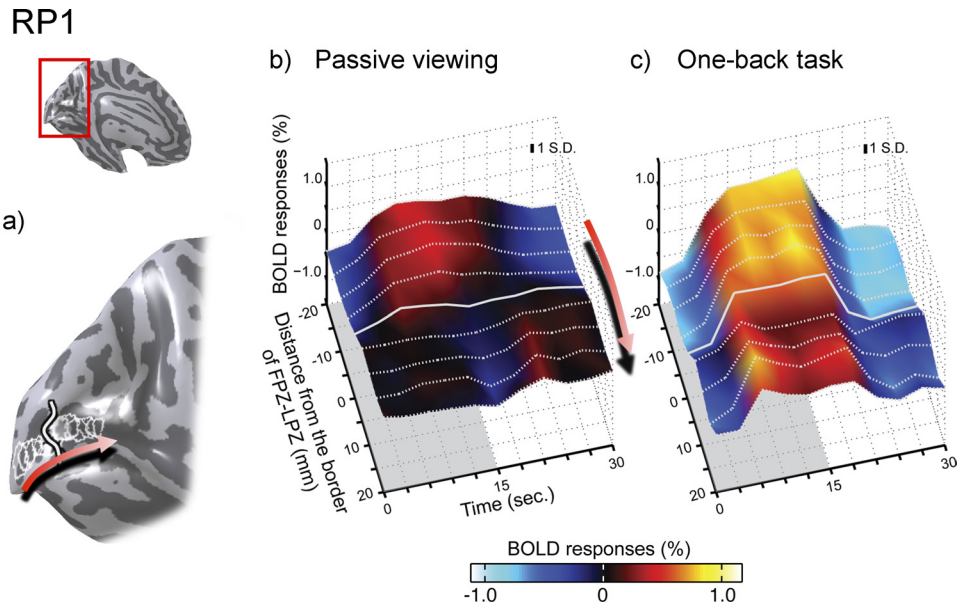


**FIGURE 3.** Single-cycle average BOLD time series within calcarine sulcus in subject RP1. (**a**) Nine circular ROIs (5-mm radius) were chosen in the calcarine sulcus of each hemisphere. The middle ROI in each hemisphere was centered on the LPZ-FPZ border; four ROIs were placed anterior and four posterior. *Red arrow*: ROIs are ordered from posterior to anterior. (**b**) Surface plot of the average single-cycle BOLD time series in the passive viewing condition. The *solid* and *dotted white lines* are the time series from each of the nine ROIs. The stimulus was presented in the first half of the cycle and replaced by a uniform field in the second half. *Red arrow*: ROI ordering. The *solid white line* is from the LPZ-FPZ border. The *gray shaded area* indicates the period when the stimulus is "on." In the FPZ, the responses increase and decrease in phase with the stimulus (positive response). In the LPZ, anterior to the border, the response is out of phase with the stimulus (negative response). (**c**) In the OBT, the LPZ responses change from negative to positive. Inflated cortical surface of the left hemisphere of the subject (*inset*, *upper left*). Typical ±1 SD for a response point is inset within the figure. Colors indicate the BOLD percent modulation around the mean response.

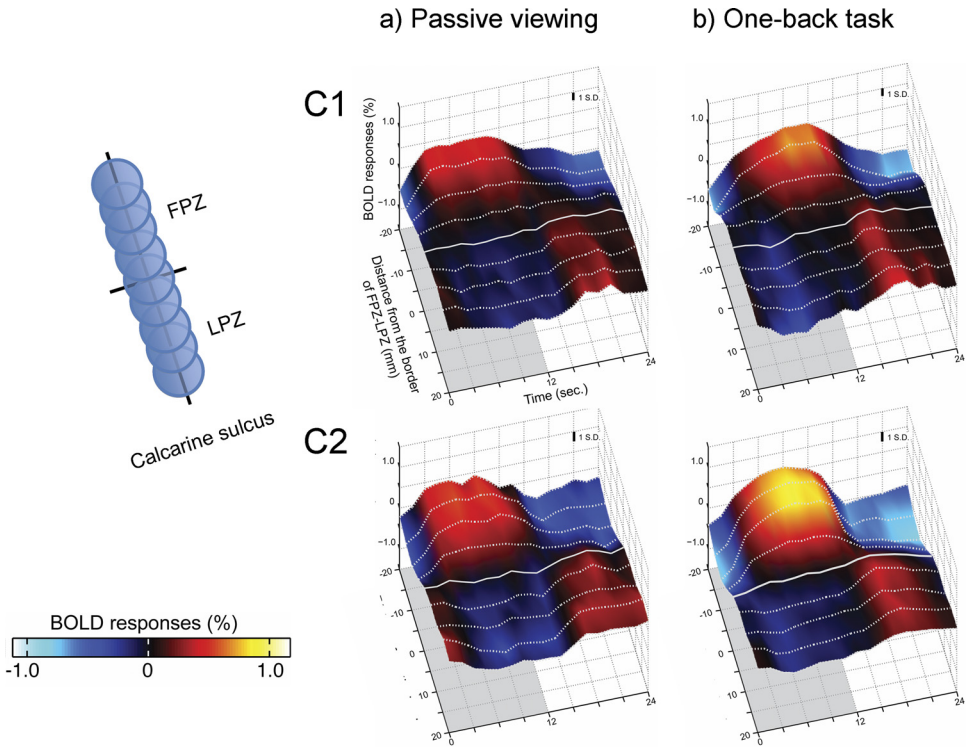


**Figure 4.** Average single-cycle BOLD time series in two controls. ROIs were created as in Figure 3. (**a**) In the passive viewing condition, BOLD responses are positive in the FPZ and negative in the LPZ, as in the RP subject. (**b**) In the OBT condition, responses in the LPZ remain negative. There is no reliable task-dependent BOLD change in the control subjects. *Inset*, *left*: ordering of the ROIs from FPZ to LPZ. Other aspects are as in Figure 3.

### V1 Spatial Response Profile

We measured the spatial profile of the response from posterior to anterior calcarine sulcus. In each hemisphere, we first created a large ROI covering the calcarine sulcus, centered on the border between the positive and the negative BOLD responses during passive viewing. We have plotted the mean response of each point in the ROI as a function of that point's distance along the cortical surface to the border (Fig. 6).

In control subjects, the response declined from the posterior to the anterior calcarine (gray-shaded area), and the decline was similar in passive viewing (Fig. 6a) and in the OBT (Fig. 6b). In RP subjects, however, the decline of the response varied between conditions (colored lines). In passive viewing, the responses were in the same range as the control data (Fig. 6a). During the OBT, the RP1–3 responses remained positive over a larger cortical distance (Fig. 6b).

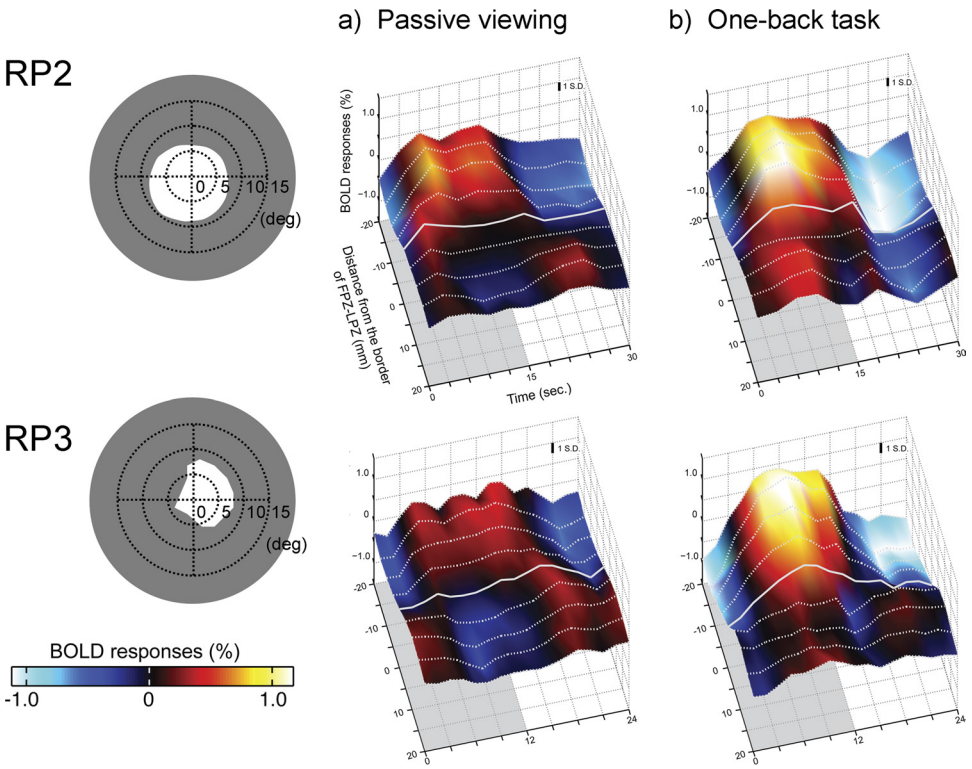


**Figure 5.** Average single-cycle BOLD time series in two additional RP subjects (RP2, RP3). *Left*: visual perimetry measurements for RP2 and RP3. (**a**) In the passive viewing condition, the BOLD responses are positive in the FPZ and negative in the LPZ, as for RP1 and the controls. (**b**) In the OBT condition, the negative responses in the LPZ become positive. Other aspects are as in Figure 3.

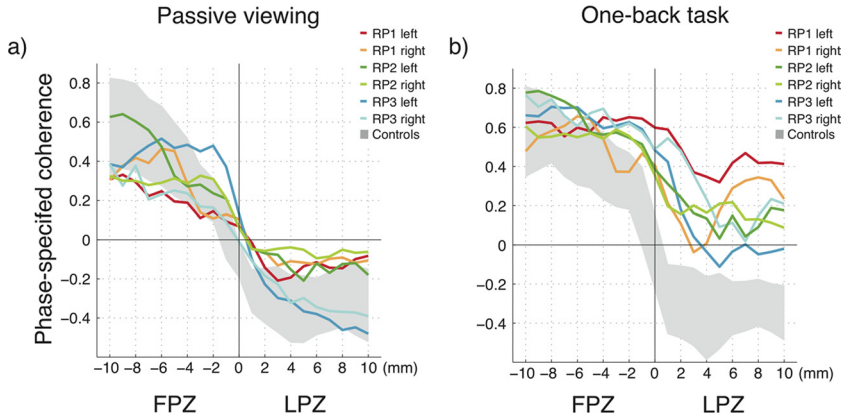


**Figure 6.** Phase-specified coherence as a function of distance from the FPZ-LPZ border. The six curves show data separately from the left and right hemispheres of the three RP subjects. *Gray-shaded area*: range of responses from the controls. Phase-specified coherence is pooled into 1-mm bins. (**a**) In the passive viewing condition, there is reasonable agreement between the RP and control responses. (**b**) In the OBT condition, the RP responses in the LPZ are significantly elevated. Further statistical analyses of these data are given in Supplementary Figure S1.

The influence of the task on BOLD responses in the controls and RP subjects is illustrated in the scatter plots in Figure 7. Each point shows the response of a voxel from the calcarine ROI in the passive (*x*-axis) and OBT (*y*-axis) conditions. For control subjects (Fig. 7a), the responses were nearly invariant between the two conditions, falling slightly above the identity line. For RP subjects (Fig. 7b), the responses differed strongly between the two conditions. The phase-specified coherence increased by approximately 0.5 as the experiment changed from passive viewing to the OBT. The positive phase-specified coherence increased by approximately 0.2.

## Discussion

While passively viewing a stimulus, RP subjects have a large zone in V1 that is either unresponsive or responsive with a negative BOLD signal. Task performance appears to add a positive, in-phase response rather than to multiply the standard responses. From these data we cannot conclude whether there has been any change over time in the size of the FPZ, though the positions of the V1 FPZ and LPZ are consistent with the size of the retinal lesion and typical V1 visual field maps.[23] However, there is no way to evaluate this question precisely because of the large biological variability in V1 size across subjects.[24]

While actively judging the same stimuli, BOLD responses in the LPZ of the RP subjects change, becoming more positive. The only difference between the passive and one-back viewing conditions is the task; the stimulus modulations are identical. Therefore, we conclude that the stimulus-synchronized responses in the LPZ are elicited by the task (which changed), not the stimulus (which did not change). Hence, the LPZ responses in anterior calcarine of the RP subjects are task-dependent, just as the LPZ responses in posterior calcarine are task-dependent in JMD subjects.

RP subject responses differ from the responses in controls. Controls also have a negative BOLD response beyond the stimulus, but there is no significant task-dependent change in the V1 response within the simulated LPZ.

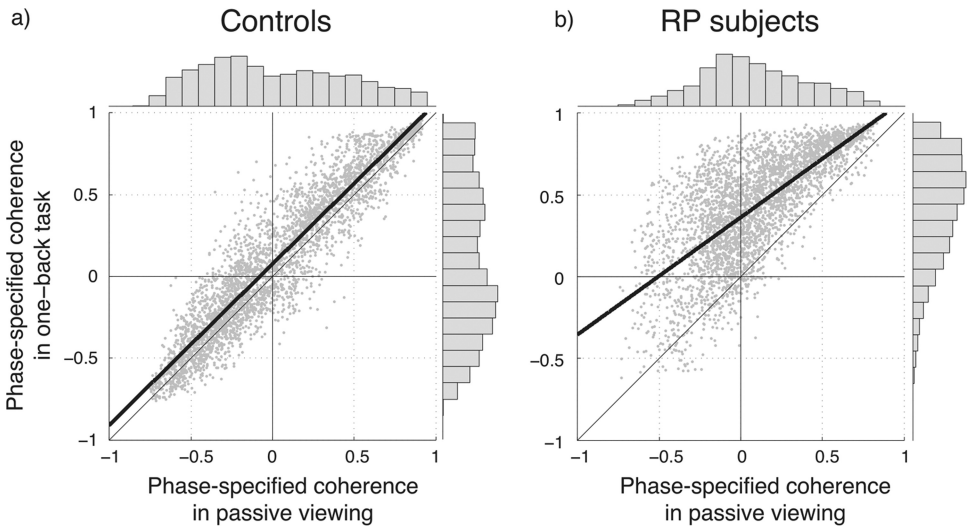


**Figure 7.** Phase-specified coherence with the stimuli compared in passive viewing and OBT conditions. Each point shows the phase-specified response of a voxel in one of the calcarine ROIs in the passive (*x*-axis) and OBT (*y*-axis) conditions. (**a**) For the two control subjects, the points fall near the identity line, showing that the responses are nearly invariant across the two conditions. (**b**) For the RP subjects, the negative BOLD responses in the passive-viewing condition become more positive in the OBT condition. In other words, the out-of-phase voxels in passive viewing turn to in-phase to the visual stimuli in OBT. Histograms showing the marginal distributions of the coherence values for passive and one-back conditions are plotted at the upper and right edges of the graphs. There is no significant difference between the distributions except for the OBT condition in RP subjects. *Heavy solid lines*: best linear-fit to the data; *thin line*: identity line. Definition of ROI is same as in Figure 6.

## Relationship to Other BOLD Measurements

Masuda et al.[2] observed a large silent LPZ during passive viewing in subjects with JMD. Although it is impossible to know whether there is a biological stimulus-driven response below the signal-to-noise ratio of the measurement method, we can say that any such response is very small compared with the response in healthy cortex. In addition, any potential stimulus-driven BOLD response is smaller than the task-dependent response, which is easily measured.

There have been many reports of attention-related BOLD responses in primary visual cortex.[25–27] Recent reports in animal models confirm that the BOLD response is induced by anticipation of a signal rather than the signal itself.[28]

Baker et al.[29] report a BOLD response in the LPZ of JMD subjects. This phenomenon is unlike the measurements described here and those by Masuda et al.[2] in two ways. First, the BOLD responses are not adjacent to the FPZ-LPZ border; rather they are separated by more 1 to 3 cm. Second, the modulations they describe do not require the subject to perform a task and can be measured in passive viewing.[30] The responses described by Baker et al.[29] differ from those of an earlier report[1] and have been disputed by a second group.[31]

## Relationship to Electrophysiology

There is a large number of publications describing the effect of retinal lesions on neural responses in LGN and V1. These papers contain many contradictory findings that are reviewed in Wandell et al.[3] Some groups assert that reorganization requires deletion of signals from both eyes; other groups say that reorganization can be found after deletion of signals from one eye.[32–38] Some groups assert that there is an enormous expansion of receptive field size and orientation tuning after the lesion; others do not.[32,33,39] There is wide divergence between groups on the estimated time course of the putative reorganization.[32,36,38,40–43] There are also different views about the degree of reorganization at different locations within the visual pathways.[41,42,44–48] Finally, all these studies are limited because they follow only population responses without a model of population statistics, and none follow the responses of individual receptive fields over time.[3]

## Visual Mechanisms

V1 neuron receptive fields span a distance of several millimeters, and the spatial distribution of feed-forward and feed-back signals differ considerably.[49–53] For example, the receptive field size of the feed-back signals from MT to V1 projection field is ~27° in macaque.[49,53] Such a large V1 receptive field from extrastriate cortex may be the source of the signals in the LPZ.

To explain these differences, we expand on the hypothesis that task-related LPZ responses in JMD subjects arise because the retina fails to deliver a key signal to the geniculo-striate pathway.[2] In controls, the healthy retina in the region of the simulated scotoma provides a signal indicating that there is zero contrast (Fig. 8). This zero-contrast signal also gates the extrastriate feed-back signal into V1, and no net BOLD response is produced. In JMD patients, the zero-contrast retinal signal is absent. This produces an unusual condition: there is neither a primary signal into V1 nor a signal to gate the extrastriate feed-back. In the absence of the gating signal, extrastriate signals enter V1 and produce a BOLD response that is not observed in controls.

This model explains the BOLD responses as an unmasking of cortical feed-back that is normally present but is blocked from entering V1 by the gating mechanism. The difference between controls and subjects with retinal dysfunction is explained by the deletion of the gating signal, and we would not describe the deletion of an existing signal as large-scale reorganization.[29,30] Rather, this model only assumes that (a) there are extrastriate gating signals from the LGN and that (b) these gating signals are missing in retinal disease. In other respects, the circuitry is unchanged.

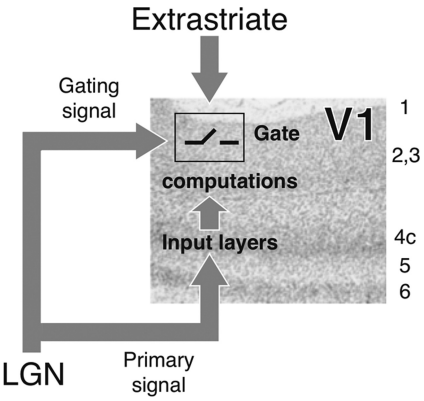


**FIGURE 8.** A model of V1 circuitry to explain task-dependent BOLD modulations in MD and RP subjects. Primary signals from the LGN project to the main input layers in V1. The LGN also sends a gating signal that governs the effectiveness of extrastriate signals. When there is very low retinal image contrast, the primary signal from the LGN is noise. The LGN gating signal prevents extrastriate feed-back from interacting with the noise transmitted to V1. When there is reliable retinal contrast, the primary signal is meaningful and the LGN gating signal allows extrastriate signals to pass through and interact. When a retinal region is dysfunctional, both the primary signal and the gating signal are absent. Without the gating signal, extrastriate signals can be transmitted into V1 even in the absence of a primary signal from the LGN. In this case, the extrastriate signals produced a BOLD response that was not present in controls.

## Implications for Retinal and Visual Therapy

There are no effective treatments for patients with retinal degeneration; however, many important genes have been identified and their functions have been elucidated, providing potential for gene-based treatments.[54] There are recent exciting reports of gene therapy in patients with Leber's congenital amaurosis.[55–58] These therapies are limited to the mutations in the *RPE65* gene, but the method should generalize to other types of mutations.[54,59,60] Three general types of visual prostheses are proposed for patients with human retinal degeneration: retinal,[61–66] optic nerve,[67–69] and cortical.[70–73] In the future, stem cell therapy may repopulate degenerated retinas.[74,75] These visual therapies are not yet widely used, but there is hope for all of them.

Suppose that after retinal dystrophy new cortical synapses develop. In that case, therapies that replace the dysfunctional retinal signals would rely on deletion of these new synapses, or at least on reduction in their efficacy, to render the new therapeutic inputs useful. Alternatively, there may be no substantial change in the circuit connectivity, but there may be a powerful increase in specific synaptic signals that carry feed-back and lateral connections. Again, for the therapy to be effective, it would require a downregulation of these signals. Finally, suppose that there is no new circuit development or large upregulation; rather the BOLD responses are increased only because deletion of the feed-forward signals unmasks the existing feed-back. In that case, simply replacing the missing inputs with new cells or prosthetic signals would be sufficient to restore vision.

Each of these cases has different clinical implications. If one accepts the idea of new circuit development, it seems likely

that the reorganization in each patient will differ. It also seems likely that the cortex of only some patients will be able to reorganize a second time and take advantage of the signals provided by the new therapy. The success of the new therapy may depend on identifying those patients who have a reversible reorganization and those who do not. If no new circuits develop but there is a strong upregulation of existing synaptic connections, then it may be necessary for the therapy to convert the state of these upregulated synapses back to their proper strength. Finally, if there is no substantial reorganization and the functional circuits are simply lying fallow, then the signals delivered by the therapy will find fertile ground and vision should be restored.

The work described in this article suggests that cortical rewiring is not essential to explain the BOLD responses in LPZ and that the main difference we observe in subjects with retinal dystrophies can be explained by preexisting circuits that are missing an important component (retinal input) or possibly by upregulation of the feed-back circuits.

There remain many important questions that need further exploration. If the normal feed-back signals are enhanced by retinal dysfunction, is this an impediment to vision and restoration therapies? We also wonder whether the degree of retinal loss may influence the likelihood of cortical reorganization. For example, the degree of reorganization may vary if the retinal ganglion cells remain alive and there is some residual signal compared with diseases that cause ganglion cell death. Combining BOLD measurements in humans with further physiological measurements in animal models should be helpful in guiding the development of retinal therapies.

## *Acknowledgments*

The authors thank Jonathan Winawer, Andreas Rauschecker, L. Michael Perry, Kendrick Kay, Alison Kevan, Shigeyuki Kan, Takahiko Koike, Kunihiro Asakawa, Kaoru Amano, Kibo Yoshida, Hiroshi Tsuneoka, and Kenji Kitahara for their help and for comments on this manuscript.

## *References*

1. Sunness JS, Liu T, Yantis S. Retinotopic mapping of the visual cortex using functional magnetic resonance imaging in a patient with central scotomas from atrophic macular degeneration. *Ophthalmology.* 2004;111:1595–1598.
2. Masuda Y, Dumoulin SO, Nakadomari S, Wandell BA. V1 projection zone signals in human macular degeneration depend on task, not stimulus. *Cereb Cortex.* 2008;18:2483–2493.
3. Wandell BA, Smirnakis SM. Plasticity and stability of visual field maps in adult primary visual cortex. *Nat Rev Neurosci.* 2009;10:873–884.
4. Baseler H, Gouws A, Crossland M, et al. Large-scale cortical reorganization is absent in both juvenile and age-related macular degeneration. *J Vis.* 2009;9:733.
5. Daiger SP, Bowne SJ, Sullivan LS. Perspective on genes and mutations causing retinitis pigmentosa. *Arch Ophthalmol.* 2007;125:151–158.
6. Hartong DT, Berson EL, Dryja TP. Retinitis pigmentosa. *Lancet.* 2006;368:1795–1809.
7. Bhatti MT. Retinitis pigmentosa, pigmentary retinopathies, and neurologic diseases. *Curr Neurol Neurosci Rep.* 2006;6:403–413.
8. Hamel CP. Cone rod dystrophies. *Orphanet J Rare Dis.* 2007;2:7.
9. Brainard DH. The psychophysics toolbox. *Spat Vis.* 1997;10:433–436.
10. Pelli DG. The VideoToolbox software for visual psychophysics: transforming numbers into movies. *Spat Vis.* 1997;10:437–442.
11. Glover GH, Lai S. Self-navigated spiral fMRI: interleaved versus single-shot. *Magn Reson Med.* 1998;39:361–368.
12. Glover GH. Simple analytic spiral K-space algorithm. *Magn Reson Med.* 1999;42:412–415.
13. Wandell BA, Chial S, Backus BT. Visualization and measurement of the cortical surface. *J Cogn Neurosci.* 2000;12:739–752.
14. Nestares O, Heeger DJ. Robust multiresolution alignment of MRI brain volumes. *Magn Reson Med.* 2000;43:705–715.
15. Bandettini PA, Jesmanowicz A, Wong EC, Hyde JS. Processing strategies for time-course data sets in functional MRI of the human brain. *Magn Reson Med.* 1993;30:161–173.
16. Logothetis NK, Wandell BA. Interpreting the BOLD signal. *Annu Rev Physiol.* 2004;66:735–769.
17. Liu J, Wandell BA. Specializations for chromatic and temporal signals in human visual cortex. *J Neurosci.* 2005;25:3459–3468.
18. Teo PC, Sapiro G, Wandell BA. Creating connected representations of cortical gray matter for functional MRI visualization. *IEEE Trans Med Imaging.* 1997;16:852–863.
19. Brewer AA, Liu J, Wade AR, Wandell BA. Visual field maps and stimulus selectivity in human ventral occipital cortex. *Nat Neurosci.* 2005;8:1102–1109.
20. Wade AR, Brewer AA, Rieger JW, Wandell BA. Functional measurements of human ventral occipital cortex: retinotopy and colour. *Philos Trans R Soc Lond B Biol Sci.* 2002;357:963–973.
21. Grill-Spector K, Malach R. The human visual cortex. *Annu Rev Neurosci.* 2004;27:649–677.
22. Kanwisher N. Faces and places: of central (and peripheral) interest. *Nat Neurosci.* 2001;4:455–456.
23. Dougherty RF, Koch VM, Brewer AA, Fischer B, Modersitzki J, Wandell BA. Visual field representations and locations of visual areas V1/2/3 in human visual cortex. *J Vision.* 2003;3:586–598.
24. Stensaas SS, Eddington DK, Dobelle WH. The topography and variability of the primary visual cortex in man. *J Neurosurg.* 1974;40:747–755.
25. O'Craven KM, Rosen BR, Kwong KK, Treisman A, Savoy RL. Voluntary attention modulates fMRI activity in human MT-MST. *Neuron.* 1997;18:591–598.
26. Ress D, Backus BT, Heeger DJ. Activity in primary visual cortex predicts performance in a visual detection task. *Nat Neurosci.* 2000;3:940–945.
27. Brefczynski JA, DeYoe EA. A physiological correlate of the 'spotlight' of visual attention. *Nat Neurosci.* 1999;2:370–374.
28. Sirotin YB, Das A. Anticipatory haemodynamic signals in sensory cortex not predicted by local neuronal activity. *Nature.* 2009;457:475–479.
29. Baker CI, Peli E, Knouf N, Kanwisher NG. Reorganization of visual processing in macular degeneration. *J Neurosci.* 2005;25:614–618.
30. Baker CI, Dilks DD, Peli E, Kanwisher N. Reorganization of visual processing in macular degeneration: replication and clues about the role of foveal loss. *Vision Res.* 2008;48:1910–1919.
31. Baseler HA, Gouws A, Morland AB. The organization of the visual cortex in patients with scotomata resulting from lesions of the central retina. *Neuro-Ophthalmology.* 2009;33:149–157.
32. Chino YM, Kaas JH, Smith EL 3rd, Langston AL, Cheng H. Rapid reorganization of cortical maps in adult cats following restricted deafferentation in retina. *Vision Res.* 1992;32:789–796.
33. Chino YM, Smith EL 3rd, Kaas JH, Sasaki Y, Cheng H. Receptive-field properties of deafferentiated visual cortical neurons after topographic map reorganization in adult cats. *J Neurosci.* 1995;15:2417–2433.
34. Kaas JH, Krubitzer LA, Chino YM, Langston AL, Polley EH, Blair N. Reorganization of retinotopic cortical maps in adult mammals after lesions of the retina. *Science.* 1990;248:229–231.
35. Murakami I, Komatsu H, Kinoshita M. Perceptual filling-in at the scotoma following a monocular retinal lesion in the monkey. *Vis Neurosci.* 1997;14:89–101.
36. Calford MB, Schmid LM, Rosa MG. Monocular focal retinal lesions induce short-term topographic plasticity in adult cat visual cortex. *Proc Biol Sci.* 1999;266:499–507.
37. Calford MB, Wang C, Taglianetti V, Waleszczyk WJ, Burke W, Dreher B. Plasticity in adult cat visual cortex (area 17) following circumscribed monocular lesions of all retinal layers. *J Physiol.* 2000;524(pt 2):587–602.
38. Schmid LM, Rosa MG, Calford MB, Ambler JS. Visuotopic reorganization in the primary visual cortex of adult cats following mon-

ocular and binocular retinal lesions. *Cereb Cortex.* 1996;6:388–405.

39. Giannikopoulos DV, Eysel UT. Dynamics and specificity of cortical map reorganization after retinal lesions. *Proc Natl Acad Sci U S A.* 2006;103:10805–10810.
40. Heinen SJ, Skavenski AA. Recovery of visual responses in foveal V1 neurons following bilateral foveal lesions in adult monkey. *Exp Brain Res.* 1991;83:670–674.
41. Gilbert CD, Wiesel TN. Receptive field dynamics in adult primary visual cortex. *Nature.* 1992;356:150–152.
42. Darian-Smith C, Gilbert CD. Topographic reorganization in the striate cortex of the adult cat and monkey is cortically mediated. *J Neurosci.* 1995;15:1631–1647.
43. Schmid LM, Rosa MG, Calford MB. Retinal detachment induces massive immediate reorganization in visual cortex. *Neuroreport.* 1995;6:1349–1353.
44. Eysel UT. Maintained activity, excitation and inhibition of lateral geniculate neurons after monocular deafferentation in the adult cat. *Brain Res.* 1979;166:259–271.
45. Eysel UT, Gonzalez-Aguilar F, Mayer U. A functional sign of reorganization in the visual system of adult cats: lateral geniculate neurons with displaced receptive fields after lesions of the nasal retina. *Brain Res.* 1980;181:285–300.
46. Eysel UT, Gonzalez-Aguilar F, Mayer U. Late spreading of excitation in the lateral geniculate nucleus following visual deafferentation is independent of the size of retinal lesions. *Brain Res.* 1981;204:189–193.
47. Eysel UT. Functional reconnections without new axonal growth in a partially denervated visual relay nucleus. *Nature.* 1982;299:442–444.
48. Eysel UT, Neubacher U. Recovery of function is not associated with proliferation of retinogeniculate synapses after chronic deafferentation in the dorsal lateral geniculate nucleus of the adult cat. *Neurosci Lett.* 1984;49:181–186.
49. Angelucci A, Levitt JB, Walton EJ, Hupe JM, Bullier J, Lund JS. Circuits for local and global signal integration in primary visual cortex. *J Neurosci.* 2002;22:8633–8646.
50. Angelucci A, Bressloff PC. Contribution of feedforward, lateral and feedback connections to the classical receptive field center and extra-classical receptive field surround of primate V1 neurons. *Prog Brain Res.* 2006;154:93–120.
51. Angelucci A, Levitt JB, Lund JS. Anatomical origins of the classical receptive field and modulatory surround field of single neurons in macaque visual cortical area V1. *Prog Brain Res.* 2002;136:373–388.
52. Cavanaugh JR, Bair W, Movshon JA. Nature and interaction of signals from the receptive field center and surround in macaque V1 neurons. *J Neurophysiol.* 2002;88:2530–2546.
53. Harrison LM, Stephan KE, Rees G, Friston KJ. Extra-classical receptive field effects measured in striate cortex with fMRI. *NeuroImage.* 2007;34:1199–1208.
54. Smith AJ, Bainbridge JW, Ali RR. Prospects for retinal gene replacement therapy. *Trends Genet.* 2009;25:156–165.
55. Bainbridge JW, Smith AJ, Barker SS, et al. Effect of gene therapy on visual function in Leber's congenital amaurosis. *N Engl J Med.* 2008;358:2231–2239.
56. Maguire AM, Simonelli F, Pierce EA, et al. Safety and efficacy of gene transfer for Leber's congenital amaurosis. *N Engl J Med.* 2008;358:2240–2248.
57. Hauswirth WW, Aleman TS, Kaushal S, et al. Treatment of Leber congenital amaurosis due to RPE65 mutations by ocular subretinal injection of adeno-associated virus gene vector: short-term results of a phase I trial. *Hum Gene Ther.* 2008;19:979–990.
58. Cideciyan AV, Aleman TS, Boye SL, et al. Human gene therapy for RPE65 isomerase deficiency activates the retinoid cycle of vision but with slow rod kinetics. *Proc Natl Acad Sci U S A.* 2008;105:15112–15117.
59. Jacobson SG, Cideciyan AV, Aleman TS, et al. Leber congenital amaurosis caused by an RPGRIP1 mutation shows treatment potential. *Ophthalmology.* 2007;114:895–898.
60. Cideciyan AV, Swider M, Aleman TS, et al. ABCA4 disease progression and a proposed strategy for gene therapy. *Hum Mol Genet.* 2009;18:931–941.
61. Margalit E, Maia M, Weiland JD, et al. Retinal prosthesis for the blind. *Surv Ophthalmol.* 2002;47:335–356.
62. Humayun MS, Weiland JD, Fujii GY, et al. Visual perception in a blind subject with a chronic microelectronic retinal prosthesis. *Vision Res.* 2003;43:2573–2581.
63. Chow AY, Chow VY, Packo KH, Pollack JS, Peyman GA, Schuchard R. The artificial silicon retina microchip for the treatment of vision loss from retinitis pigmentosa. *Arch Ophthalmol.* 2004;122:460–469.
64. Fujikado T, Morimoto T, Kanda H, et al. Evaluation of phosphenes elicited by extraocular stimulation in normals and by suprachoroidal-transretinal stimulation in patients with retinitis pigmentosa. *Graefes Arch Clin Exp Ophthalmol.* 2007;245:1411–1419.
65. Winter JO, Cogan SF, Rizzo JF 3rd. Retinal prostheses: current challenges and future outlook. *J Biomater Sci Polym Ed.* 2007;18:1031–1055.
66. Ameri H, Ratanapakorn T, Ufer S, Eckhardt H, Humayun MS, Weiland JD. Toward a wide-field retinal prosthesis. *J Neural Eng.* 2009;6:035002.
67. Veraart C, Raftopoulos C, Mortimer JT, et al. Visual sensations produced by optic nerve stimulation using an implanted self-sizing spiral cuff electrode. *Brain Res.* 1998;813:181–186.
68. Veraart C, Wanet-Defalque MC, Gerard B, Vanlierde A, Delbeke J. Pattern recognition with the optic nerve visual prosthesis. *Artif Organs.* 2003;27:996–1004.
69. Delbeke J, Oozeer M, Veraart C. Position, size and luminosity of phosphenes generated by direct optic nerve stimulation. *Vision Res.* 2003;43:1091–1102.
70. Brindley GS, Lewin WS. The sensations produced by electrical stimulation of the visual cortex. *J Physiol.* 1968;196:479–493.
71. Dobelle WH, Mladejovsky MG, Girvin JP. Artificial vision for the blind: electrical stimulation of visual cortex offers hope for a functional prosthesis. *Science.* 1974;183:440–444.
72. Dobelle WH. Artificial vision for the blind by connecting a television camera to the visual cortex. *ASAIO J.* 2000;46:3–9.
73. Troyk P, Bak M, Berg J, et al. A model for intracortical visual prosthesis research. *Artif Organs.* 2003;27:1005–1015.
74. Mooney I, LaMotte J. A review of the potential to restore vision with stem cells. *Clin Exp Optom.* 2008;91:78–84.
75. Lamba DA, Gust J, Reh TA. Transplantation of human embryonic stem cell-derived photoreceptors restores some visual function in Crx-deficient mice. *Cell Stem Cell.* 2009;4:73–79.